# Imine-linked porous polymer frameworks with high small gas (H2, CO2, CH4, C2H2) uptake and CO 2/N2 selectivity

**ARTICLE** *in* CHEMISTRY OF MATERIALS · MAY 2013

Impact Factor: 8.35 · DOI: 10.1021/cm400019f



**3 AUTHORS:**

Youlong Zhu
University of Colorado Boulder
**11** PUBLICATIONS **246** CITATIONS
SEE PROFILE

Hai Long
National Renewable Energy Laboratory
**37** PUBLICATIONS **777** CITATIONS
SEE PROFILE

Wei Zhang
Tohoku University
**351** PUBLICATIONS **5,265** CITATIONS
SEE PROFILE

CHEMISTRY OF MATERIALS

Article

pubs.acs.org/cm

# Imine-Linked Porous Polymer Frameworks with High Small Gas ($H_2$, $CO_2$, $CH_4$, $C_2H_2$) Uptake and $CO_2/N_2$ Selectivity

Youlong Zhu,[†] Hai Long,[‡] and Wei Zhang*[,†]

[†]Department of Chemistry and Biochemistry, University of Colorado, Boulder, Colorado 80309, United States

[‡]National Renewable Energy Laboratory, Golden, Colorado 80401, United States

Supporting Information

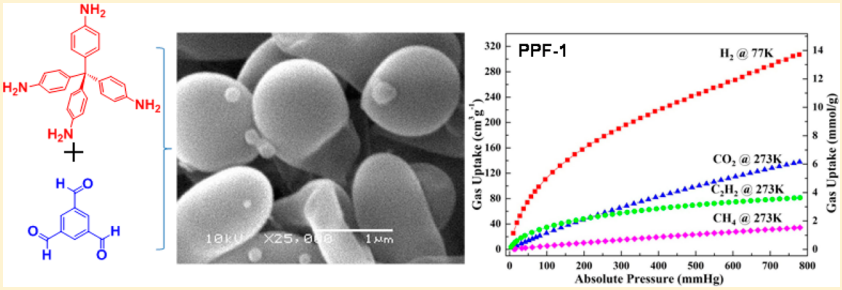


**ABSTRACT:** A series of novel porous polymer frameworks (PPFs) with [3 + 4] structure motif have been synthesized from readily accessible building blocks via imine condensation, and the dependence of gas adsorption properties on the building block dimensions and functionalities was studied. The resulting imine-linked frameworks exhibit high surface area: the Brunauer–Emmett–Teller (BET) specific surface area up to 1740 $m^2$ $g^{-1}$, and a Langmuir surface area up to 2157 $m^2$ $g^{-1}$. More importantly, the porous frameworks exhibit outstanding $H_2$ (up to 2.75 wt %, 77 K, 1 bar), $CO_2$ (up to 26.7 wt %, 273 K, 1 bar), $CH_4$ (up to 2.43 wt %, 273 K, 1 bar), and $C_2H_2$ (up to 17.9 wt %, 273 K, 1 bar) uptake, which are among the highest reported for organic porous materials. PPFs exhibit good ideal selectivities for $CO_2/N_2$ (14.5/1–20.4/1), and $CO_2/CH_4$ adsorption (8.6/1–11.0/1), and high thermal stabilities (up to 500 °C), thus showing a great potential in gas storage and separation applications.

**KEYWORDS:** *Schiff-base chemistry, organic porous polymer, small gas uptake, adsorption selectivity*

## INTRODUCTION

Recently, there has been explosive growth in the research of novel porous materials, which have shown great promise for applications in gas storage and separation. Porous materials play key roles in carbon capture and sequestration technology, and safe storage of clean energy (e.g., hydrogen) and explosive industrial gases (e.g., acetylene). A notable achievement in porous materials research is the development of porous metal–organic frameworks (MOFs),[1] highly ordered crystalline materials constructed through reticular chemistry from metal ions or clusters and organic linkers. Several of these fascinating materials have the highest surface area and gas uptake capacity reported so far among all porous materials. However, despite the great flexibility in design and phenomenal success in synthesis of highly diverse 3-D structures, MOFs invariably contain a large amount of metal centers and relatively labile coordination bonds that may limit their applications. Recently purely organic porous materials have received increasing attention and they have shown great potential in a variety of applications, such as gas storage and separation,[2] catalysis,[3] chemical sensing,[4] etc. Two types of organic porous materials have been developed in the past decade, including discrete porous organic molecules[5] and infinite porous organic polymer networks such as crystalline COFs,[6] PIMs,[7] CTFs,[8] PAFs,[9] PPNs,[10] CMPs[11] and OCFs,[12] etc. Both of these two types of materials are constructed from lightweight elements through strong covalent bonding. These materials generally possess permanent porosity, low mass densities, synthetic diversification, and high physicochemical stability, which make them highly competitive in gas storage and separation applications.[2d,10b,13]

Although significant progress has been made in the area of organic porous materials, only limited dimensionality, framework connectivity, and topologies of these promising materials have been explored. In addition, better understanding on the effect of building block features on the target framework structures and properties is still highly desired. Continuing our effort of seeking high-performance organic porous materials,[5c,12,14] we have developed high-yielding and cost-effective syntheses of a series of porous polymer frameworks (PPFs) through imine condensation, which show high $H_2$, $CO_2$, $CH_4$, and $C_2H_2$ storage capacity as well as good $CO_2/N_2$ and $CO_2/CH_4$ adsorption selectivity. The structure–property relationship was studied using various building blocks of different size

**Received:** January 3, 2013
**Revised:** April 2, 2013

   dx.doi.org/10.1021/cm400019f | *Chem. Mater.* XXXX, XXX, XXX–XXX

and functionality. Doubling the size of the aldehyde building block produced a PPF with surface area decreased by 75%. We found decoration of the framework PPF-1 with electron-donating groups enhanced the uptake of $C_2H_2$ significantly, from 9.4 to 17.9 wt %, which is the highest $C_2H_2$ capacity reported so far for organic porous materials, and comparable or superior to those of MOFs.

## RESULTS AND DISCUSSION

A few chemical transformations have been applied to the syntheses of organic porous materials, among which Schiff-base chemistry is the most widely used. We choose imine condensation reaction to connect the building blocks for the following reasons: (1) imine condensation is an efficient well-established process and does not require expensive catalysts; (2) the reversibility of the reaction offers error-correction features, thus possibly producing highly ordered crystalline materials; (3) it can introduce imine bonds into the structure that can promote $CO_2$ binding. Since, in general, 3-D frameworks provide higher surface area compared to 2-D frameworks, we searched a potential candidate 3-D topology in Reticular Chemistry Structure Resource (RCSR) database. A highly symmetric *ctn* topological structure,[15] which can be constructed from tritopic and tetratopic building blocks, appeared to be an interesting target (Scheme 1a). Although various examples of porous polymers or covalent organic frameworks (COFs) have been prepared through imine condensation,[3c,16] surprisingly, the [3 + 4] structure motif has never been explored. We used tetra-4-anilylmethane as the tetratopic building block. In order to investigate the structure−property relationship, we chose a series of trialdehydes (**2**−**5**) with different sizes (distance between two aldehyde moieties ranging from 4.99 Å to 12.37 Å) as the tritopic building blocks (Scheme 1). It has been reported that attempts to increase the pore sizes of topologically identical MOFs by using lager organic linkers commonly result in interpenetration, leading to porosity decrease.[17] One of our goals is to explore the effect of geometrical features of building blocks on the pore size distribution and surface area of these purely organic frameworks with [3 + 4] motif. 1,3,5-Triformylphloroglucinol (**3**) was synthesized as the analogue of aldehyde **2** to study the influence of hydroxyl substituents on the gas adsorption properties.

PPFs were synthesized in good yields (81−89%) by reacting 3 equiv of tetraamine **1** with 4 equiv of various trialdehydes (**2**−**5**) in a 1:1 (v/v) mixture of 1,4-dioxane and mesitylene, in the presence of 6 M acetic acid under solvothermal conditions. Multiple attempts to synthesize crystalline frameworks failed, and all materials were obtained as amorphous solids, as shown in the powder X-ray diffraction (Figures S11−S14 in the Supporting Information). Preparation of crystalline COF materials is not trivial and usually requires enormous efforts in screening of various reaction conditions.

The structures of PPFs were characterized by FT-IR and solid state NMR. FT-IR spectra of PPF-1, PPF-3, and PPF-4 show the characteristic C═N stretching band around 1623 $cm^{-1}$, which is overlapped with the aromatic ring stretching band around 1589 $cm^{-1}$ (Figures S7−S10 in the Supporting Information). The $^{13}C$ cross-polarization magic angle spinning (CP-MAS) NMR spectra of PPF-1, PPF-3, and PPF-4 showed the imine carbon resonance around 157 ppm, supporting the imine bond formation (Figures S54, S56, and S57 in the Supporting Information). There exist incompletely converted

**Scheme 1. (a) *ctn* Topological Structure from Trigonal Building Blocks and Tetrahedral Building Blocks, (b) Building Blocks for PPFs, and (c) Syntheses of PPF Series**

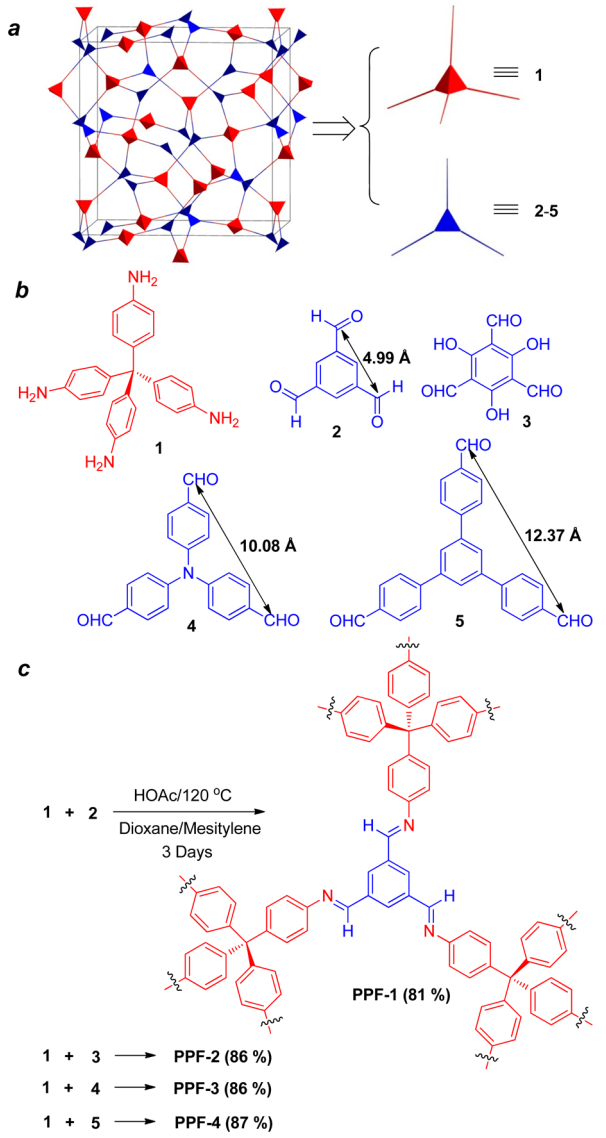


free amine and aldehyde functional groups, evidenced by the N−H stretching band around 3442 $cm^{-1}$, C═O stretching band around 1700 $cm^{-1}$ in the IR spectra, and aldehyde carbon resonance around 189 ppm in the $^{13}C$ NMR spectra.

For PPF-2, there are two possible tautomers, enol−imine form PPF-2a or keto−enamine form PPF-2b, which might coexist under equilibrium (Scheme 2). Interestingly, the $^{13}C$ CP-MAS NMR spectrum of PPF-2 shows a negligible imine carbon resonance peak around 157 ppm (Figure S55 in the Supporting Information), which is present in other imine-linked frameworks PPF-1, PPF-3, and PPF-4. It suggests that PPF-2 exists predominantly as the keto−enamine form instead of the enol−imine form. The appearance of new resonance peaks around 184 and 107 ppm in the $^{13}C$ CP-MAS NMR spectrum of PPF-2, which are characteristic resonances of carbonyl carbon and $\alpha$-carbon of keto−enamine isomer, further supports that PPF-2b is the predominant tautomer in the solid state. The IR spectrum of PPF-2 shows a strong absorption band at 1578 $cm^{-1}$ arising from C═C stretching, together with


dx.doi.org/10.1021/cm400019f | *Chem. Mater.* XXXX, XXX, XXX−XXX

**Scheme 2. Tautomerization of PPF-2**

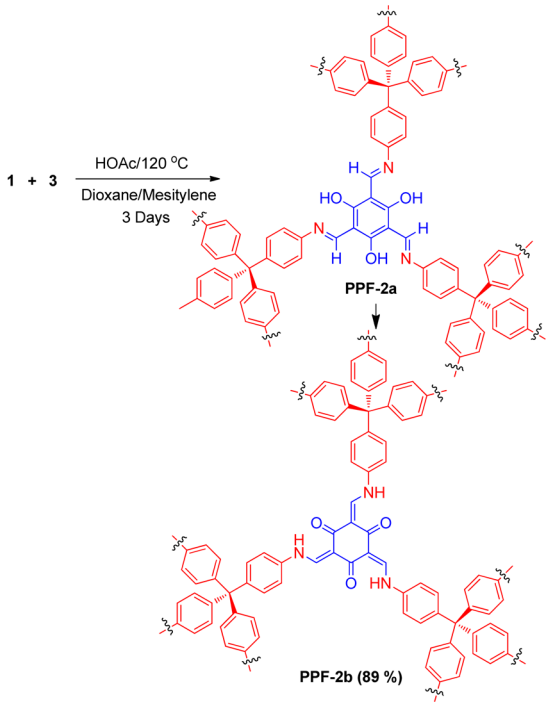


the C═O stretching band at 1616 $cm^{-1}$ and aromatic ring stretching band around 1595 $cm^{-1}$ as broad shoulders, further supporting the keto−enamine form of PPF-2.

We also performed theoretical calculations using DFT by Gaussian 09 C.01 at the B3LYP/6-311++G(2d,p) level to optimize the structure and compare their relative energies of simple model compound **6**. The computer calculations show that the keto−enamine form **6b** is totally flat and 13.9 kcal/mol more stable than the enol−imine form **6a** (Scheme 3). Our modeling study is consistent with the characterization data and X-ray crystal structure of a similar compound (**6**, $R$ = $^{t}$BOC) reported by MacLachlan, in which only the keto−enamine form was observed in both solution and the solid state.[18] Given such significant energy difference between two tautomers, and the absence of imine characters in the IR and NMR spectra,

**Scheme 3. Tautomers of Model Compound 6 (Top), and Their Energy-Minimized Structures (Bottom)**

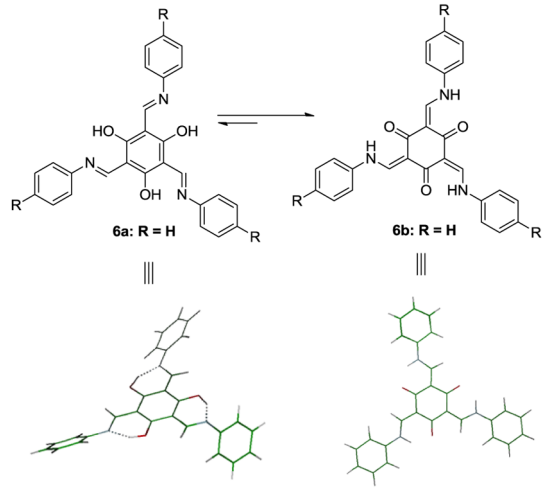


irreversible transformation of PPF-2a to PPF-2b is suggested. The IR and $^{13}$C NMR spectra of framework PPF-2b match well with the reported data of the similar 2-D COF TpPa-1 and TpPa-2 constructed from 1,3,5-triformylphloroglucinol (**3**) and *p*-phenylenediamine or 2,5-dimethyl-*p*-phenylenediamine, respectively.[19]

All the frameworks are stable under ambient conditions, and we did not observe any decomposition during purification and handling. Scanning electron microscopy (SEM) images showed that PPF-1 consists of mostly uniform sea anemone-shaped particles, whereas PPF-2, PPF-3, and PPF-4 are composed of particles of various sizes, ranging from a hundred nanometers to several micrometers (Figure 1). The materials are insoluble in

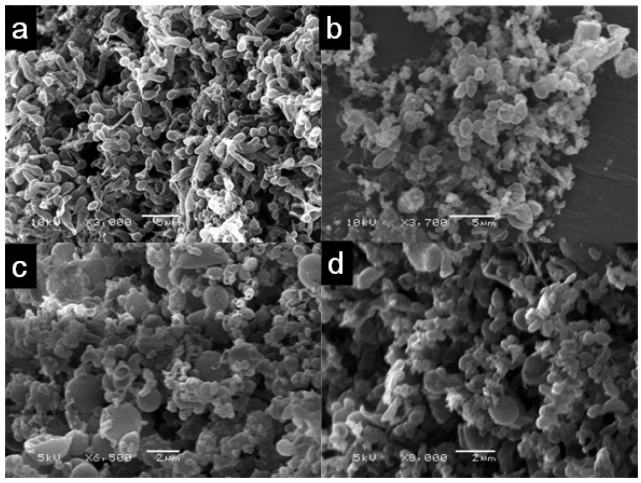


**Figure 1.** SEM images of PPF-1 (a), PPF-2 (b), PPF-3 (c), and PPF-4 (d).

most common organic solvents. PPF-1, PPF-3, and PPF-4 showed superior thermal stability with the onset decomposition temperatures >501 °C (Figure S1 in the Supporting Information). PPF-2 decomposes at relatively lower temperature (400 °C).

The permanent porosities of PPF-1−PPF-4 were characterized by nitrogen adsorption/desorption isotherms of freshly activated samples at 77 K. The fully reversible adsorption−desorption of nitrogen depicted in Figure 2 shows type I isotherm character with a rapid uptake at low relative pressure ($P/P_0$ = 0−0.1), indicating a permanent microporosity nature of all the PPFs. According to the IUPAC classification, all of the

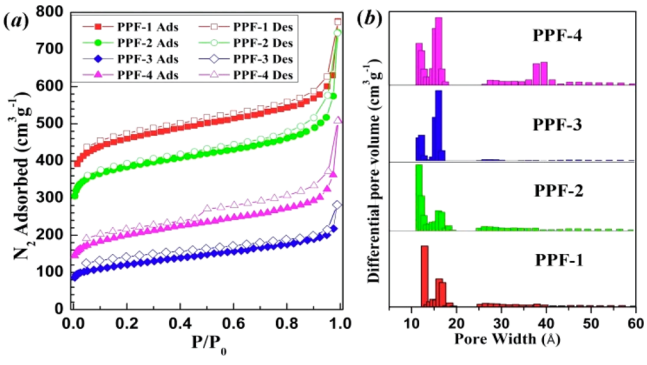


**Figure 2.** (a) $N_2$ adsorption (solid) and desorption (hollow) isotherms of PPFs at 77 K; (b) pore size distribution of PPF series.


dx.doi.org/10.1021/cm400019f | *Chem. Mater.* XXXX, XXX, XXX−XXX

PPFs are typical microporous materials.[20] The gradual increase in nitrogen adsorption under relatively high pressure ($P/P_0$ = 0.1−0.9) and the sharp increase above $P/P_0$ = 0.9 are presumably due to the presence of interparticular void.[21] The isotherms in the low relative pressure range ($P/P_0$ = 0−0.1) show decrease in $N_2$ uptake in the order of PPF-1 > PPF-2 > PPF-4 > PPF-3. The pore size distribution (PSD) analysis based on the nonlocal density functional theory (NLDFT) model shows that smaller micropores (pore width < 1.5 nm) are dominant in PPF-1 and PPF-2, whereas relatively larger micropores (pore width > 1.5 nm) are predominant in PPF-3 and PPF-4, and there is a significant amount of mesopores in PPF-4. In general, the micropore size distribution of PPFs is shifted to the larger pores when larger building blocks are used. These results indicate that the pore size distribution of these frameworks can be controlled by varying the size of building blocks.

All the PPFs showed a small hysteresis in the whole range of relative pressure suggesting relatively strong gas binding on the pore surface. The $N_2$ isotherms of PPF-4 show both type I and type IV character with significant hysteresis, consistent with the presence of a pronounced amount of mesopores. The calculated Brunauer−Emmett−Teller (BET) specific surface areas of the PPF series are 1740 $m^2\ g^{-1}$, 1470 $m^2\ g^{-1}$, 419 $m^2\ g^{-1}$, and 726 $m^2\ g^{-1}$ for PPF-1, PPF-2, PPF-3, and PPF-4 respectively, and the Langmuir surface areas are 2157 $m^2\ g^{-1}$, 1918 $m^2\ g^{-1}$, 598 $m^2\ g^{-1}$, and 1162 $m^2\ g^{-1}$, respectively (corresponding to $P/P_0$ = 0.4) (Table 1). These surfaces are comparable or higher than previously reported organic porous materials constructed through imine condensation.

**Table 1. Summary of Porosity and Pore Volume for PPF Series**

| polymer | $SA_{BET}$[a] | $SA_{Lang}$[b] | $V_{total}$[c] |
|---|---|---|---|
| PPF-1 | 1740 | 2157 | 1.18 |
| PPF-2 | 1470 | 1918 | 1.14 |
| PPF-3 | 419 | 598 | 0.37 |
| PPF-4 | 726 | 1162 | 0.77 |

[a]Surface area ($m^2\ g^{-1}$) calculated from the nitrogen adsorption based on the BET model. [b]Surface area ($m^2\ g^{-1}$) calculated from the nitrogen adsorption isotherms based on the Langmuir model. [c]The total pore volume ($cm^3\ g^{-1}$) calculated at $P/P_0$ = 0.99.

It is interesting to note that the surface area was dramatically decreased (from $SA_{BET}$ 1740 $m^2\ g^{-1}$ of PPF-1 to 419 $m^2\ g^{-1}$ of PPF-3) when the size of the aldehyde building block was increased from 4.99 Å to 10.08 Å (distance between two aldehyde moieties). The network entanglement might be one possible reason for this porosity decrease. It has been documented that interpenetration occurs commonly, thus reducing the effective size of the pores, when large building blocks are used to increase the pore dimensions.[10a] One such example is the imine-linked 3D COF-300, reported by Yaghi.[22] However, when even larger aldehyde building block **5** (the distance between two aldehyde moieties is 12.37 Å) was used, we observed an increase in surface area (from $SA_{BET}$ 419 $m^2\ g^{-1}$ to 726 $m^2\ g^{-1}$). The structure of aldehyde **5** shares the same geometrical features as aldehyde **4** with an $sp^2$-hybridization planar configuration for the nitrogen atom and propeller-like arrangement for the three phenyl rings. Therefore, similar building block connectivity in PPF-3 and PPF-4 is assumed. SEM images of PPF-3 and PPF-4 show similar morphological features, both consisting of mostly spheres of various sizes. One possible reason could be that the reduced aldehyde reactivity of tris(4-formylpheny)amine (**4**) toward imine condensation and more labile imine bond of PPF-3 could produce more structure defects in the framework. However, due to the lack of more detailed 3-D structural information on these amorphous materials, the reason for lowest surface area of PPF-3 is still open to speculation.

Given the microporous nature and the narrow pore size distribution of the PPF series, we next investigated their gas uptake capacities of small molecules ($CO_2$, $H_2$, $CH_4$, and $C_2H_2$) (Figure 3). In general, increased gas uptake capacities were

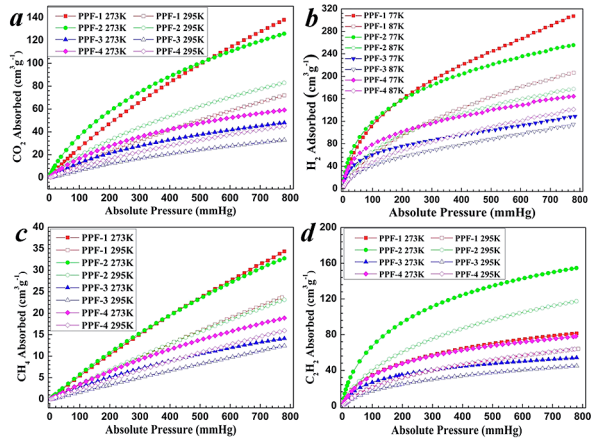


**Figure 3.** (a) $CO_2$ adsorption of PPF series at 273 K and 295 K. (b) $H_2$ adsorption of PPF series at 77 K and 87 K. (c) $CH_4$ adsorption of PPF series at 273 K and 295 K. (d) $C_2H_2$ adsorption of PPF series at 273 K and 295 K.

observed with increased porosity, i.e., uptakes of $CO_2$, $H_2$, and $CH_4$ are in the order of PPF-1 > PPF-2 > PPF-4 > PPF-3, consistent with the order of $SA_{BET}$ of these frameworks. PPF-1 with highest $SA_{BET}$ adsorbs 136 $cm^3\ g^{-1}$ (26.7 wt %) of $CO_2$ at 273 K and 1 bar; 305 $cm^3\ g^{-1}$ (2.75 wt %) of $H_2$ at 77 K and 1 bar; and 34 $cm^3\ g^{-1}$ (2.43 wt %) of $CH_4$ at 273 K and 1 bar. To our knowledge, the adsorption capacities of PPF-1 toward $CO_2$, $H_2$, and $CH_4$ are among the highest in all organic porous materials that have been reported (see Table 3), and even competitive with the best reported MOFs under the same conditions (Mg-MOF-74 has been reported to have the highest $CO_2$ adsorption capacity of 27.5 wt % at 298 K and 1 bar).[23] At 195 K and 1 bar, the $CO_2$ uptake reached an impressive amount of 444 $cm^3\ g^{-1}$ (87.2 wt %) (Figure S16 in the Supporting Information). PPF-2 also shows excellent gas adsorption capabilities, albeit it adsorbs slightly less $CO_2$, $H_2$, and $CH_4$ compared to PPF-1 under the same conditions. The $CO_2$, $H_2$, and $CH_4$ uptake of PPF-3 and PPF-4 are almost reduced by half under identical conditions, compared to PPF-1 and PPF-2, which is consistent with their significantly reduced specific surface areas.

In addition to $CO_2$, $H_2$, and $CH_4$ storage by porous materials, extensive research efforts have been devoted to acetylene ($C_2H_2$) storage. Acetylene is the most common starting material in various industries, such as the petrochemical industry, and serves as an important building block in organic syntheses. Acetylene is also considered as an important alternative energy source. However, acetylene is explosive when it is compressed to above 30 psi at room temperature


dx.doi.org/10.1021/cm400019f | Chem. Mater. XXXX, XXX, XXX−XXX

**Table 2. Summary of Gas Adsorption Properties of PPF Series at Low Pressure**

| | $CO_2$ uptake[a] | | $H_2$ uptake[b] | | $CH_4$ uptake[a] | | $C_2H_2$ uptake[a] | | selectivity[c] | |
|---|---|---|---|---|---|---|---|---|---|---|
| porous polymer | wt % | $Q_{st}$ | wt % | $Q_{st}$ | wt % | $Q_{st}$ | wt % | $Q_{st}$ | $CO_2/N_2$ | $CO_2/CH_4$ |
| PPF-1 | 26.7 | 25.6 | 2.75 | 6.8 | 2.43 | 15.1 | 9.38 | 27.9 | 14.5 | 11.0 |
| PPF-2 | 24.4 | 29.2 | 2.28 | 7.5 | 2.31 | 15.9 | 17.9 | 31.6 | 15.4 | 10.6 |
| PPF-3 | 9.2 | 21.8 | 1.14 | 8.2 | 1.00 | 19.4 | 6.23 | 29.7 | 20.4 | 9.2 |
| PPF-4 | 11.4 | 25.1 | 1.47 | 8.1 | 1.32 | 13.9 | 8.97 | 23.9 | 15.0 | 8.6 |

[a]273 K, 1 bar; unit of $Q_{st}$: kJ mol$^{-1}$. [b]77 K, 1 bar; unit of $Q_{st}$: kJ mol$^{-1}$. [c]Adsorption selectivity at 273 K and 1 bar.

**Table 3. Summary of Gas Adsorption Properties of Organic Porous Materials at Low Pressure**

| | | | | $CO_2$ uptake[c] | | $H_2$ uptake[d] | | |
|---|---|---|---|---|---|---|---|---|
| porous polymer | $SA_{BET}$[a] | $SA_{Lang}$[a] | $V_{pore}$[b] | wt % | $Q_{st}$ | wt % | $Q_{st}$ | ref |
| PPF-1 | 1740 | 2157 | 1.18 | 26.7 | 25.6 | 2.75 | 6.8 | this work |
| BILP-4 | 1135 | 1486 | 0.65 | 23.5 | 28.7 | 2.30 | 7.8 | 13a |
| CPOP-1 | 2220 | 2508 | 1.293 | 21.2 | 27.0 | 2.80 | N/A | 2d |
| PAF-3 | 2932 | 3857 | 1.54 | 15.3 | 19.2 | 2.07 | 6.6 | 24 |
| COF-102 | 3620 | 4650 | 1.55 | 5.3 | N/A | 1.20 | N/A | 25 |
| A1-B2 | 1521 | N/A | 1.13 | N/A | N/A | 1.50 | 3.0 | 16c |

[a]Unit: m$^2$ g$^{-1}$. [b]Unit: cm$^3$ g$^{-1}$. [c]273 K, 1 bar; unit of $Q_{st}$: kJ mol$^{-1}$, [d]77 K, 1 bar; unit of $Q_{st}$: kJ mol$^{-1}$.

even in the absence of oxygen. The safe storage and transportation of acetylene gas in porous materials is recommended as a promising technology.[26] However, only limited organic porous materials have been reported for acetylene adsorption. Our frameworks showed excellent $C_2H_2$ adsorption capacities (6.23−17.9 wt %) at 273 K and 1 bar. The impressive $C_2H_2$ uptake of 17.9 wt % in PPF-2 is the highest reported so far for all organic porous materials. Although our experimental data suggests that the $CO_2$, $H_2$, and $CH_4$ uptakes are proportional to the surface area (PPF-1 is the highest), interestingly, PPF-2 shows the highest $C_2H_2$ uptake (153 cm$^3$ g$^{-1}$ at 273 K and 1 bar), almost 2-fold higher than PPF-1 (80 cm$^3$ g$^{-1}$). Given the structural similarity of PPF-1 and PPF-2, the increased acetylene adsorption is presumably due to the electron-donating substituents in framework PPF-2. The stronger polarizing effect induced by carbonyls and secondary amines in PPF-2 presumably enables its stronger interactions with $C_2H_2$.[27] It has been reported that electron-rich benzene rings have stronger C−H···$\pi$ interactions with acetylene compared to electron-deficient ones.[28]

To further understand the gas adsorption properties, the isosteric heats ($Q_{st}$) of adsorption for different gases were calculated from the gas adsorption isotherms at two different temperatures by fitting the data to virial equation (Figure 3 and Figures S21−S53 in the Supporting Information). A summary of $Q_{st}$ for different gases were shown in Table 2. Among these frameworks, the highest $Q_{st}$ for $CO_2$ (29.2 kJ mol$^{-1}$) and $C_2H_2$ (31.6 kJ mol$^{-1}$) were observed for PPF-2, and the highest $Q_{st}$ for $H_2$ (8.2 kJ mol$^{-1}$) and $CH_4$ (19.4 kJ mol$^{-1}$) were observed for PPF-3 at zero coverage. All of these $Q_{st}$ values are highest among reported values for organic porous polymers and comparable to some MOF compounds.[10a,25,29] The impressive isosteric heat of 31.6 kJ/mol further indicates the strong interaction of PPF-2 with acetylene guest molecule. It should be noted that PPF-2, the functionalized analogue of PPF-1, generally shows higher $Q_{st}$ than unfunctionalized PPF-1, which supports the notion that incorporating polar groups inside the pore surface can enhance the gas binding of porous materials.[2c,13b]

To assess the potential applications of these frameworks in postcombustion $CO_2$ capture under ambient pressure, single-component gas adsorption isotherms were carried out on $CO_2$ and $N_2$ under 273 K and up to 780 mmHg (Figure 4). $CO_2/N_2$

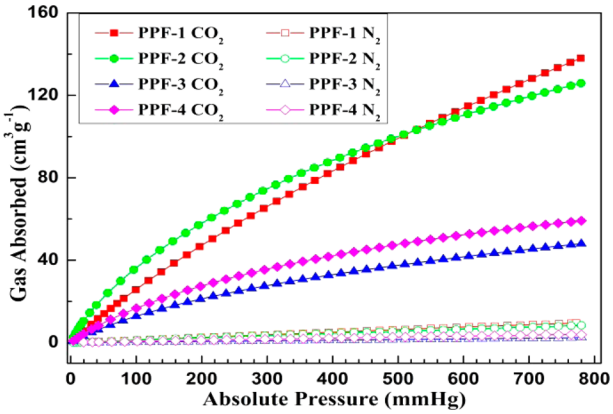


**Figure 4.** Single-component gas adsorption isotherms for $CO_2$ and $N_2$ at 273 K.

selectivities were calculated by using the ideal adsorption solution theory (IAST)[30] method at 273 K and 1 bar. Good $CO_2$ over $N_2$ adsorption selectivities (14.5, 15.4, 20.4, and 15.0) were observed for PPF-1, PPF-2, PPF-3, and PPF-4, respectively (Table 2). High $CO_2$ adsorption capacity as well as $CO_2/N_2$ adsorption selectivities are the two key parameters for evaluating the potential of porous materials in carbon dioxide capture applications. PPFs also showed good adsorption selectivities (8.6−11.0) toward $CO_2$ over $CH_4$ at 273 K and 1 bar, further highlighting the great potential of these PPFs in gas separation applications.

## CONCLUSION

We have successfully synthesized a series of microporous polymer frameworks with novel [3 + 4] structure motif through the imine condensation. The BET surface area of these PPFs is up to 1740 m$^2$ g$^{-1}$. Owing to the narrow pore size distribution and electron-rich pore surface, PPFs exhibit exceptionally high


dx.doi.org/10.1021/cm400019f | Chem. Mater. XXXX, XXX, XXX−XXX

$H_2$ uptake of up to 2.75 wt % (77 K and 1 bar), $C_2H_2$ uptake of 17.9 wt % (273 K and 1 bar), and $CO_2$ uptake of 26.7 wt % (273 K and 1 bar). Moreover, PPFs show a good $CO_2/N_2$ adsorption ideal selectivity (up to 20.4/1), as well as $CO_2/CH_4$ selectivity (up to 11.0/1), at 273 K and 1 bar. The gas adsorption properties strongly depend on the building block size and functionalities. We observed 75% decrease in surface area when the size of the aldehyde building block was doubled. Introduction of the hydroxyl functional group to the building block design increased the $C_2H_2$ uptake of the framework. Collectively, size and functional group dependent characteristics along with the relatively low cost for large-scale manufacturing of these porous polymers open a possibility for tailoring properties and preparing organic porous polymers highly competitive in gas storage and separation applications. Extended research of this series of materials is ongoing in our lab.

## ■ ASSOCIATED CONTENT

### Supporting Information

Detailed experimental materials, general synthetic routes for tetra-4-anilylmethane and PPF series; TGA, FT-IR spectrum, additional gas adsorption properties, solid state NMR spectra, SEM images (PDF). This material is available free of charge via the Internet at http://pubs.acs.org.

## ■ AUTHOR INFORMATION


### Corresponding Author

*E-mail: wei.zhang@colorado.edu.


### Notes

The authors declare no competing financial interest.

## ■ ACKNOWLEDGMENTS

The authors thank National Science Foundation (IIP-1230142), the MAST center, and 3M Non-Tenured Faculty Award for financial support, Dr. Bret A. Voss for XRD and TGA measurements, Dr. Richard Shoemaker for his assistance in solid-state NMR experiments, and Dr. Yinghua (Alice) Jin for her help with SEM characterization and manuscript preparation. This research used capabilities of the National Renewable Energy Laboratory Computational Sciences Center, which is supported by the Office of Energy Efficiency and Renewable Energy of the U.S. Department of Energy under Contract No. DE-AC36-08GO28308.

## ■ REFERENCES


(1) Zhou, H. C.; Long, J. R.; Yaghi, O. M. *Chem. Rev.* **2012**, *112*, 673.

(2) (a) Wood, C. D.; Tan, B.; Trewin, A.; Su, F.; Rosseinsky, M. J.; Bradshaw, D.; Sun, Y.; Zhou, L.; Cooper, A. I. *Adv. Mater.* **2008**, *20*, 1916. (b) Han, S. S.; Furukawa, H.; Yaghi, O. M.; Goddard, W. A. *J. Am. Chem. Soc.* **2008**, *130*, 11580. (c) Dawson, R.; Adams, D. J.; Cooper, A. I. *Chem. Sci.* **2011**, *2*, 1173. (d) Chen, Q.; Luo, M.; Hammershoj, P.; Zhou, D.; Han, Y.; Laursen, B. W.; Yan, C. G.; Han, B. H. *J. Am. Chem. Soc.* **2012**, *134*, 6084.

(3) (a) Wang, C.; Xie, Z. G.; deKrafft, K. E.; Lin, W. B. *ACS Appl. Mater. Interfaces* **2012**, *4*, 2288. (b) Xie, Z. G.; Wang, C.; deKrafft, K. E.; Lin, W. B. *J. Am. Chem. Soc.* **2011**, *133*, 2056. (c) Ding, S. Y.; Gao, J.; Wang, Q.; Zhang, Y.; Song, W. G.; Su, C. Y.; Wang, W. *J. Am. Chem. Soc.* **2011**, *133*, 19816.

(4) Zhao, C.; Danish, E.; Cameron, N. R.; Kataky, R. *J. Mater. Chem.* **2007**, *17*, 2446.

(5) (a) Tozawa, T.; et al. *Nat. Mater.* **2009**, *8*, 973. (b) Tian, J.; Thallapally, P. K.; Dalgarno, S. J.; McGrail, P. B.; Atwood, J. L. *Angew. Chem., Int. Ed.* **2009**, *48*, 5492. (c) Jin, Y. H.; Voss, B. A.; Noble, R. D.; Zhang, W. *Angew. Chem., Int. Ed.* **2010**, *49*, 6348.

(6) (a) Feng, X.; Ding, X.; Jiang, D. *Chem. Soc. Rev.* **2012**, *41*, 6010. (b) Cote, A. P.; Benin, A. I.; Ockwig, N. W.; O'Keeffe, M.; Matzger, A. J.; Yaghi, O. M. *Science* **2005**, *310*, 1166. (c) El-Kaderi, H. M.; Hunt, J. R.; Mendoza-Cortes, J. L.; Cote, A. P.; Taylor, R. E.; O'Keeffe, M.; Yaghi, O. M. *Science* **2007**, *316*, 268. (d) Spitler, E. L.; Colson, J. W.; Uribe-Romo, F. J.; Woll, A. R.; Giovino, M. R.; Saldivar, A.; Dichtel, W. R. *Angew. Chem., Int. Ed.* **2012**, *51*, 2623.

(7) Wood, C. D.; et al. *Chem. Mater.* **2007**, *19*, 2034.

(8) (a) Kuhn, P.; Antonietti, M.; Thomas, A. *Angew. Chem., Int. Ed.* **2008**, *47*, 3450. (b) Kuhn, P.; Forget, A.; Su, D. S.; Thomas, A.; Antonietti, M. *J. Am. Chem. Soc.* **2008**, *130*, 13333. (c) Ren, S. J.; Bojdys, M. J.; Dawson, R.; Laybourn, A.; Khimyak, Y. Z.; Adams, D. J.; Cooper, A. I. *Adv. Mater.* **2012**, *24*, 2357.

(9) (a) Ben, T.; et al. *Angew. Chem., Int. Ed.* **2009**, *48*, 9457. (b) Ren, H.; Ben, T.; Wang, E. S.; Jing, X. F.; Xue, M.; Liu, B. B.; Cui, Y.; Qiu, S. L.; Zhu, G. S. *Chem. Commun.* **2010**, *46*, 291.

(10) (a) Lu, W. G.; et al. *Chem. Mater.* **2010**, *22*, 5964. (b) Yuan, D. Q.; Lu, W. G.; Zhao, D.; Zhou, H. C. *Adv. Mater.* **2011**, *23*, 3723.

(11) (a) Jiang, J. X.; et al. *Angew. Chem., Int. Ed.* **2007**, *46*, 8574. (b) Jiang, J. X.; et al. *Angew. Chem., Int. Ed.* **2008**, *47*, 1167.

(12) Jin, Y. H.; Voss, B. A.; McCaffrey, R.; Baggett, C. T.; Noble, R. D.; Zhang, W. *Chem. Sci.* **2012**, *3*, 874.

(13) (a) Rabbani, M. G.; El-Kaderi, H. M. *Chem. Mater.* **2012**, *24*, 1511. (b) Lu, W. G.; Yuan, D. Q.; Sculley, J. L.; Zhao, D.; Krishna, R.; Zhou, H. C. *J. Am. Chem. Soc.* **2011**, *133*, 18126.

(14) Jin, Y. H.; Voss, B. A.; Jin, A.; Long, H.; Noble, R. D.; Zhang, W. *J. Am. Chem. Soc.* **2011**, *133*, 6650.

(15) O'Keeffe, M.; Peskov, M. A.; Ramsden, S. J.; Yaghi, O. M. *Acc. Chem. Res.* **2008**, *41*, 1782.

(16) (a) Schwab, M. G.; Fassbender, B.; Spiess, H. W.; Thomas, A.; Feng, X. L.; Mullen, K. *J. Am. Chem. Soc.* **2009**, *131*, 7216. (b) Uribe-Romo, F. J.; Hunt, J. R.; Furukawa, H.; Klock, C.; O'Keeffe, M.; Yaghi, O. M. *J. Am. Chem. Soc.* **2009**, *131*, 4570. (c) Pandey, P.; Katsoulidis, A. P.; Eryazici, I.; Wu, Y. Y.; Kanatzidis, M. G.; Nguyen, S. T. *Chem. Mater.* **2010**, *22*, 4974. (d) Laybourn, A.; Dawson, R.; Clowes, R.; Iggo, J. A.; Cooper, A. I.; Khimyak, Y. Z.; Adams, D. J. *Polym. Chem.* **2012**, *3*, 533. (e) Jin, Y.; Zhu, Y.; Zhang, W. *CrystEngComm* **2013**, *15*, 1484.

(17) Yaghi, O. M. *Nat. Mater.* **2007**, *6*, 92.

(18) Chong, J. H.; Sauer, M.; Patrick, B. O.; MacLachlan, M. J. *Org. Lett.* **2003**, *5*, 3823.

(19) Kandambeth, S.; Mallick, A.; Lukose, B.; Mane, N. V.; Heine, T.; Banerjee, R. *J. Am. Chem. Soc.* **2012**, *134*, 19524.

(20) Rouquerol, J.; Avnir, D.; Fairbridge, C. W.; Everett, D. H.; Haynes, J. H.; Pernicone, N.; Ramsay, J. D. F.; Sing, K. S. W.; Unger, K. K. *Pure Appl. Chem.* **1994**, *66*, 1739.

(21) Weber, J.; Schmidt, J.; Thomas, A.; Bohlmann, W. *Langmuir* **2010**, *26*, 15650.

(22) Uribe-Romo, F. J.; Hunt, J. R.; Furukawa, H.; Klock, C.; O'Keeffe, M.; Yaghi, O. M. *J. Am. Chem. Soc.* **2009**, *131*, 4570.

(23) Sumida, K.; Rogow, D. L.; Mason, J. A.; McDonald, T. M.; Bloch, E. D.; Herm, Z. R.; Bae, T. H.; Long, J. R. *Chem. Rev.* **2012**, *112*, 724.

(24) Ben, T.; Pei, C. Y.; Zhang, D. L.; Xu, J.; Deng, F.; Jing, X. F.; Qiu, S. L. *Energy Environ. Sci.* **2011**, *4*, 3991.

(25) Furukawa, H.; Yaghi, O. M. *J. Am. Chem. Soc.* **2009**, *131*, 8875.

(26) Zhang, Z. J.; Xiang, S. C.; Chen, B. L. *CrystEngComm* **2011**, *13*, 5983.

(27) Li, J. R.; Kuppler, R. J.; Zhou, H. C. *Chem. Soc. Rev.* **2009**, *38*, 1477.

(28) Mishra, B. K.; Karthikeyan, S.; Ramanathan, V. *J. Chem. Theory Comput.* **2012**, *8*, 1935.

(29) (a) Wang, Z. G.; Zhang, B. F.; Yu, H.; Sun, L. X.; Jiao, C. L.; Liu, W. S. *Chem. Commun.* **2010**, *46*, 7730. (b) Gallo, M.; Glossman-Mitnik, D. *J. Phys. Chem. C* **2009**, *113*, 6634.

(30) Myers, A. L.; Prausnitz, J. M. *AIChE J.* **1965**, *11*, 121.